# The Excitator as a minimal model for the coordination dynamics of discrete and rhythmic movement generation

Viktor K. Jirsa, J.A. Scott Kelso

Center for Complex Systems and Brain Sciences
Florida Atlantic University
Boca Raton, Florida 33431, USA
Corresponding author's email: jirsa@ccs.fau.edu

Accepted for publication in Journal of Motor Behavior

Running title: Excitator

April 13, 2004

**Abstract**

We identify a class of excitable two-dimensional model systems, the Excitators, which provide an entry point to the understanding of the mechanisms of discrete and rhythmic movement generation, and a variety of related phenomena such as false starts and the geometry of phase space trajectories. The starting point of our analysis is the topological properties of the phase flow. In particular, the existence of the phenomenon of false starts provides a characteristic structural condition, the separatrix, for the phase flow, which partitions the phase space. We discuss the existence of threshold phenomena, which are characteristic of excitable systems, as well as the existence of stable and unstable fixed points and periodic orbits. Our analysis predicts the existence of stable manifolds in the proximity of fixed points resulting in an overshoot and a slow return phase after movement execution. To investigate coordination phenomena, we discuss the effects of two types of couplings, the sigmoidal coupling and a truncated version thereof, known as the HKB-coupling. We show analytically and numerically that the sigmoidal coupling leads to convergence phenomena in

phase space, whereas the HKB-coupling displays convergent, as well as divergent behavior. A specific representation of the Excitator is suggested and allows the quantification of our predictions.

# 1 Introduction

How limb movements are controlled under the conditions of a changing environment may be described causally by a variety of approaches, each emphasizing different facets of the problem. Biomechanically based models approach the dynamics of limb motion utilizing the idea that muscles can behave like complex springs [Feldman, 1980a, Feldman, 1980b, Balasubramaniam & Feldman, 2004]. The flexor and extensor muscles are idealized by springs that exert forces on masses, primarily the bone of the limb. If these forces are in equilibrium, then the limb is at rest. Movement control is accomplished by changing the parameters of the mass-spring system such that the equilibrium point shifts and the now destabilized system seeks to move towards the new equilibrium point. This and closely related principles are known in the literature as equilibrium controls, in particular the $\alpha$ models [Polit & Bizzi, 1978, Polit & Bizzi, 1979] and the $\lambda$ models [Feldman, 1980a, Feldman, 1980b, Balasubramaniam & Feldman, 2004]. It is fairly well accepted that the equilibrium models provide a good account of how a joint or limb achieves its terminal position (see [Kelso, 1977, Kelso et al., 1979, Schmidt & Mc Gown, 1980]) and they are well-suited to describe discrete movement tasks. Rhythmic tasks involving the periodic joint motion between two positions would have to be described by providing a periodic equilibrium point control and hence result in an externally driven system. Another type of models, often referred to as the Dynamical Systems approach, emphasizes the importance of structures and symmetries within the dynamics of the observable and is less concerned with the identification of the material elements (muscles, tendons, etc.) underlying the observed dynamics. Examples are the Haken-Kelso-Bunz (HKB) model [Haken, Kelso, & Bunz, 1985] describing bimanual rhythmic movement coordination, the model by Schöner [Schöner , 1990], which extends the HKB model to discrete movements, and Sternad et al.'s model [Sternad et al., 2000], which is also capable of describing discrete and rhythmic movement generation. The HKB model is a system of two nonlinearly coupled limit cycle oscillators, which are realized by Van der Pol-Rayleigh oscillators. The relative phase between the two limit cycles exhibits stable in-phase and anti-phase coordination of which the latter is destabilized through a pitchfork bifurcation as the movement frequency is increased. Schöner [Schöner , 1990] suggested a modification of the intrinsic dynamics of this set of oscillators, but did not alter the coupling. The modified dynamics is based on a model by Gonzalez and Piro [Gonzalez & Piro, 1987], which displays two stable fixed points for one parameter setting, and the existence of a stable periodic orbit for another parameter setting. Movement control is achieved by changing the model parameters for specific time windows

and thus stabilizing/destabilizing the stationary solutions appropriately. Sternad et al.'s model [Sternad et al., 2000] consists of two units - one limit cycle (rhythmic) and one point attractor (discrete) unit - that are coupled by mutually inhibitory connections. Due to the coupling, step changes to the discrete unit shift the center of oscillation in a phase-dependent manner which captures the observed pattern in experimental data. From neuroscience, in particular recent fMRI studies, evidence shows that different cortical subsystems contribute to the generation of synchronized and syncopated movement [Mayville et al., 2002] in addition to a common cortical control. In particular, syncopation has been interpreted as "executed individually on each perception-action cycle" [Mayville et al., 2002], implying the character of a discrete movement. Several attempts have been made to attribute neuroscientific meaning to the model equations of the Dynamical System's approach. Grossberg and colleagues [Grossberg, Pribe, & Cohen, 1997; Pribe, Grossberg, & Cohen, 1997], as well as Nagashino & Kelso [Nagashino & Kelso, 1992], used neural oscillator equations to reproduce stabilization/destabilization phenomena of the relative phase found in bimanual coordination. Similarly, Beek and colleagues postulated the existence of an interplay between neural fields and the behavioral effectors [Beek, Peper, & Daffertshofer, 2002] to understand lag-one correlation effects as known from the continuation paradigm employed by Wing and Kristofferson [Wing & Kristofferson, 1973]. Such neural fields have been developed by Jirsa and Haken [Jirsa & Haken, 1996, Jirsa & Haken, 1997] in the context of MEG studies of sensorimotor coordination and control [Fuchs, Kelso, & Haken, 1992; Kelso, Bressler, Buchanan, DeGuzman, Ding, Fuchs, & Holroyd, 1992; Jirsa, Friedrich, Haken, & Kelso, 1994]. More general treatments of neural fields have been discussed extensively in the literature[Amari, 1977; Wilson & Cowan, 1972;Wilson & Cowan, 1973; Nunez, 1974; Nunez, 1995; Jirsa & Haken, 1996; Jirsa & Kelso, 2000; Jirsa, 2003; Wright & Liley, 1996; Robinson, Rennie, & Wright, 1997; Haken, 1996; Haken, 2002]. Following the introduction of the bimanual rhythmic coordination paradigm [Kelso, 1981], several brain imaging studies have successfully mapped the underlying spatiotemporal brain activity onto movement and coordination variables[Fuchs et al., 1992; Kelso et al., 1992; Jirsa, Friedrich, & Haken, 1995; Kelso, Fuchs, Lancaster, Holroyd, Cheyne, & Weinberg, 1998; Fuchs, Jirsa, & Kelso, 2000; Fuchs, Mayville, Cheyne, Weinberg, Deecke, & Kelso, 2000; Jirsa, 2003; Meyer-Lindenberg, Ziemann, Hajak, Cohen, & Berman, 2002]. In particular, the behavioral HKB equations were successfully derived from neural field equations [Jirsa et al., 1998, Daffertshofer et al., 2004] allowing for an interpretation of the phenomenological coupling terms.

In the present paper we wish to identify a minimal model of discrete and rhythmic movement generation, which encapsulates all the dynamic features discussed above. Phenomena such as false starts and trajectory shapes may be understood on the basis of our proposed model. We discuss the dynamics analytically and provide theoretical proof that the HKB-coupling, and generalized forms thereof, always results in a convergence or divergence of the movement patterns, in dependence of the initial limb positions only. The proof is given independent of the specific type of coordination, thus is true for both discrete and rhythmic movement patterns. Our approach emphasizes symmetry and topological arguments. However, there are several implications that hint at connections to an underlying neural basis, based primarily on the similarity between the model developed here and a variety of equations describing neuronal dynamics, such as the Fitzhugh-Nagumo system [FitzHugh, 1961]. In section 2 we discuss the intrinsic dynamics of the proposed model, followed by a discussion of the coupled dynamics of two such model systems in section 3. Section 4 summarizes and concludes this paper.

# 2 Intrinsic dynamics of the Excitator

## 2.1 Trajectory formation in phase space: Theory

A false start is the act of beginning a behavior at an inappropriate moment in time. The behavior may be fully or only partially executed. In language production, a false start is the act of beginning an utterance and typically aborting it prior to completion. False start errors occur most often when a conversation becomes intense and are used in the quantitative study of speech impairment [Croot, Hodges, Xuereb & Patterson, 2000]. In sports and movement sciences, a false start, e.g. in sprinting [Collet, 1999], is the initiation of a movement prior to the signal of the starter[1]. Many theoretical questions arise on error production and the underlying mechanisms involved in error production, detection and correction (see [Postma, 2000] for a review). For instance, Schmidt and Gordon (1977) studied the cost and benefit for anticipated movement initiation. In the present paper, we wish to focus on the mechanism for movement initiation itself and discuss various alternatives for error production, that is false movement initiation, and their implementation in terms of dynamical systems currently discussed in the literature.

[1]Note that Olympic standards allow a minimum of 100ms reaction time only. Anything faster than that is considered a false start according to Olympic regulations.

To do so, we have to formalize our definition of a false movement initiation (false start): "A system shall have the ability to perform a movement cycle as a consequence of a stimulus for a fixed set of parameters. If the system performs the same movement cycle, or partially executed forms thereof, in the absence of the external signal, then we call the movement cycle a false start." This definition of a false start implies its probabilistic character and hence is dependent on the presence and strength of fluctuations which are always present in real dissipative systems [Haken, 1983]. The notion of "intention" does not explicitly occur in our definition, but it is implicitly present as a variable that changes the likelihood of a false start. Our definition provides a minimal basis, which enables us to study some characteristic properties of false starts, but certainly is not intended to capture all aspects of a false start present in the literature.

Given the above formalization of a false start, what are possible realizations thereof in dynamic systems? In Schöner's two-dimensional model [Schöner , 1990] a discrete movement is initiated by "turning on" a "behavioral information", just long enough to get a joint or limb from a given position A to another position B in phase space. The phase space is spanned by two variables $x$ and $y$. Here $x$ may be interpreted as the position of an effector and $y$ as a variable which is related to the velocity. The behavioral information changes the phase flow topology temporarily from a structure with two stable fixed points A and B (see figure 1 a) to a limit cycle (see figure 1 c). Figure 1 shows a graphical representation of such trajectories with varying phase flow topologies. If the behavioral information does not remain "on" long enough, the system will return to point A, if it stays "on" too long, then the system actually passes point B and also returns to point A, but performs a large amplitude flexion-extension cycle first (see figure 1 b). It appears that most of the complexity of the formation of movement trajectories has been shifted into the creation of behavioral information. In particular, the occurrence of false starts raises the question of how a whole movement cycle is initiated, even though there is no intent to do so. Given the present formal definition, it seems reasonable to interpret the initiation of a false start as a stochastic process that operates close to a threshold: If the system crosses the threshold, for instance due to a larger fluctuation, then the formation of the resulting trajectory will be dominated by its deterministic features. However, the onset of a false start will have a probabilistic character that will be a function of expectation and attentional factors, which should be directly correlated with the distance of the fixed point to the threshold in phase space for a fixed noise level. On the other hand, notice that the introduction of noise and variability into the concept of behavioral information, which is the cause for the movement

initiation in the Schöner model [Schöner , 1990], would result in a whole range of behaviors from simple deviations around position A through half-cycles (AB), full cycles (ABA) and 3/2 cycles (ABAB). To narrow the range of behaviors to partial movement cycles, such as simple deviations around the fixed point, and complete movement cycles only (ABA), it would be necessary to postulate that behavioral information occurs in a quantized manner, such that it may fluctuate only within specified time windows. Not only does such a requirement seem artificial, but also it just shifts the initial question of why either no movement or a complete movement is initiated to the alternative question of why either no behavioral information is generated or only behavioral information is generated that lasts for a specific time window.

FIGURE 1 HERE

For these reasons, we choose to remain in the original two-dimensional phase space spanned by the variables $x$ and $y$ and discuss which elements must be present in order to observe the above phenomena of false starts, rhythmic and discrete movements and shape of phase space trajectories. Additional degrees of freedom may exist as has been shown by Beek et al. [Beek et al., 2002] to capture lag-one correlation effects [Wing & Kristofferson, 1973]. Such dynamics may still be captured satisfactorily by lower dimensional systems as long as the dynamics is not chaotic, since deterministic chaos requires at least three degrees of freedom [Strogatz, 1994]. This can be accomplished by identifying the two-dimensional phase space in $x$ and $y$ with a two-dimensional attractive surface in a higher dimensional space. As a consequence, any deviation from this surface will result in a dynamics back to the surface satisfying the criteria of Beek et al. [Beek et al., 2002]. However, the dynamics is reducible to a two-dimensional dynamics (for instance using techniques such as the order parameter concept of synergetics [Haken, 1983]). We choose to focus primarily on the existence of topological structures (layout of fixed points, limit cycles, etc.) rather than on details of phase space trajectories. Examples of topological structures are separatrices, which partition the phase space locally into separate regimes. A well-known example in a one-dimensional phase space is the unstable fixed point of the HKB-potential in bimanual coordination [Haken et al., 1985] separating the two stable fixed points, in-phase and anti-phase. Homeomorphisms are smooth continuous transformations from one set of variables to another that preserve the topology of the flow in phase space. Hence, to achieve a classification of dynamic systems, it is sufficient to discuss the properties of one specific system only if we are able to find a homeomorphism that maps the particular system onto a class of other systems. In fact, the class of systems will actually be defined by the specific system and

the homeomorphism. We will present examples thereof later.

Our starting point of modelling is the following: We need at least one stable fixed point in phase space, which will represent our rest position A as shown in figure 2. Second, we need some kind of barrier or threshold near this fixed point such that on one side of this barrier the flow in phase space is directed towards the fixed point, on the other side away from it. This is accomplished by means of a separatrix, which divides the local neighborhood into two distinct areas with opposite horizontal flows (see figure 2).

FIGURE TWO HERE

The separatrix introduces naturally the threshold-like properties of a false start. The existence of a separatrix is the basis of the current model. More generally, a nullcline is the graphical representation of the set of points for which either the horizontal or the vertical flow is zero. The intersection of two nullclines identifies fixed points, i.e. points with zero horizontal and vertical flow in phase space. Without loss of generality we choose the separatrix as $y = -x$ which is identical to the nullcline of the horizontal flow. The sign of the flow must be chosen to be repelling, that is

$$\dot{x} = x + y - g_1(x) \tag{1}$$

where $g_1(x)$ is a purely nonlinear function, $\partial_x g_1 = 0$ for $x = 0$, which guarantees that the trajectories remain bounded horizontally, if $g_1(x \to \pm\infty) \to \pm\infty$. A slightly stronger condition is the requirement of point symmetry, $g_1(-x) \overset{x\to\pm\infty}{\longrightarrow} -g_1(x)$ which also guarantees boundedness. Note that the previous condition is sufficient, however, since a point-symmetric function $g_1$ is often used in applications, we will use this constraint unless stated otherwise. The nullcline of the vertical flow $\dot{y}$ must generate at least one fixed point $(x_0, y_0)$ at position A in phase space, $\dot{y} = f(x_0, y_0) = 0$, which is given by the intersection of the nullclines of horizontal and vertical flow. To guarantee linear stability of the fixed point, we require for the vertical flow

$$\dot{y} = f(x, y) = \underbrace{f(x_0, y_0)}_{=0} + \underbrace{\partial_x f(x_0, y_0)}_{\leq 0}(x - x_0) + \underbrace{\partial_y f(x_0, y_0)}_{\leq 0}(y - y_0) + \text{higher orders.} \tag{2}$$

We identify $\partial_x f(x_0, y_0) = -1$, $x_0 = a$ and $g_2(x, y) = -\partial_y f(x_0, y_0)(y - y_0) + O(x^2, y^2)$ where $O(x^2, y^2)$ is the Landau symbol, which means that the term $O(x^2, y^2)$ contains polynomials of at least the second (or higher) order. With these considerations we obtain the following ordinary

differential equation

$$\begin{aligned} \dot{x} &= (x + y - g_1(x))\tau \\ \dot{y} &= -(x - a + g_2(x, y) - I)/\tau \end{aligned} \tag{3}$$

where $\tau$ is a time constant and external input $I$ is introduced via the vertical flow. The model system in equation (3) falls into the class of excitable systems, that is systems which exhibit threshold properties and return, when having crossed the threshold, to the initial position after a long transient for an appropriate choice of $g_1(x)$ and $g_2(x, y)$. Excitable systems[2] systems have been studied in various fields of science dealing with threshold elements [Strogatz, 1994], but in particular in biology as a model for neuronal functioning [Murray, 1993]. In the following we wish to refer to the model system described by equation (3) as the Excitator. To ensure the excitable properties of the Excitator in equation (3), the following constraints, which are derived in appendix A, have to be satisfied:

$$\begin{array}{lccc} \text{Existence of separatrix:} & \partial_x g_1(0) = 0 & & \\ \text{Stability of fixed point } (x_0, y_0): & \partial_x g_1 > 1 & \partial_y g_2(\partial_x g_1 - 1) + \partial_x g_2 + 1 > 0 & \\ \text{Boundedness } (x, y \gg 1): & g_1(-x) \overset{x\to\pm\infty}{\longrightarrow} -g_1(x) & G(-y) \overset{y\to\pm\infty}{\longrightarrow} -G(y) & \\ & & G(y) = g_1^{-1}(y) - a + g_2(g_1^{-1}(y), y) & \end{array} \tag{4}$$

where the partial differentials in the constraint for the stability of the fixed point $(x_0, y_0)$ have to be evaluated at the fixed point. The time constant $\tau$ should be chosen to be large, $\tau \gg 1$, to guarantee sufficiently fast horizontal flow away from the separatrix. Actually, in practice, it turns out that $\tau \geq 1$ is fully sufficient. Under these conditions $x$ becomes a fast variable and $y$ a slow variable resulting in a sequentially occurring time scale hierarchy. Such systems are referred to in the literature as relaxation oscillators, e.g. the FitzHugh-Nagumo system [FitzHugh, 1961], the Hodgkin-Huxley equations [Hodgkin & Huxley, 1952], the Hindmarsh-Rose oscillator [Hindmarsh & Rose, 1982] and the Van-der-Pol oscillator (see e.g. [Perko, 1991]). These dynamic systems typically have a parameter regime in which limit cycle behavior exists. This can be easily shown by applying the Poincaré-Bendixson theorem (e.g. [Haken, 1983]), which states that a stable limit cycle exists if a closed region may be found in the phase space, such that the flow at the boundaries of the region points inside and the region does not contain any fixed points. The boundedness criterion of equation (4) guarantees an outer boundary with inwards flow. An inner boundary, its flow and the fixed points will depend on the details of

[2]Excitable systems are not to be confused with excited or self-excited systems. The former refer to systems with an external driver, the latter refer to systems with a self-excitation term, typically negative damping.

the functions $g_1(x), g_2(x,y)$. The primary purpose of $g_1(x)$ is to guarantee the boundedness of the system dynamics along the $x$-direction, whereas $g_2(x,y)$ identifies the task conditions. In particular, the expression $-a+g_2(x,y)$ will be used to implement the task constraints (see below for explicit examples) reflected in the topology of the phase flow.

A notable feature of the phase plane trajectories is that the sequential time scale hierarchy, $x$ being a faster variable compared to $y$, creates an attractive manifold in phase space, if the system is sufficiently far away from the separatrix. In this region, the different time scales allow one to eliminate the fast variable $x$ by means of adiabatic elimination [Haken, 1983], $\dot{x} = 0$. We thereby obtain a reduced description of the dynamics,

$$y \approx g_1(x) \tag{5}$$

and

$$\dot{y} = -(g_1^{-1}(y) - a + g_2(g_1^{-1}(y), y) - I)/\tau \tag{6}$$

as long as the system dwells in this region of phase space. Along this "return manifold" the trajectory returns from an overshoot and moves toward a stable fixed point or just defines a segment on the left and right hand side of the limit cycle in phase space (see section 2.2 for illustrations thereof). The inverse of $g_1(x)$ must exist only locally in phase space, that is in the region of interest. Experimental and theoretical examples are presented in section 2.2.

A simple realization of the Excitator, which satisfies all conditions in equation (4), is given by $g_1(x) = x^3/3$ and results in the following dynamic system

$$\begin{aligned} \dot{x} &= (x + y - 1/3x^3)\tau \\ \dot{y} &= -(x - a + by - I)/\tau \end{aligned} \tag{7}$$

where the three task conditions are defined by the parameters $a$ and $b$: (I) *bistable* ($a = 0, b = 2$); (II) *monostable* ($a = 1.05, b = 0$); (III) *limit cycle* ($a = 0, b = 0$). The nullclines of the two-dimensional flow, $y = -x + (1/3)x^3$ for the horizontal flow and $x = a - g_2(x,y)$ for the vertical flow, are plotted in figure 3 for the three different conditions. The intersections of the nullclines define the stable and unstable fixed points.

FIGURE THREE HERE

The monostable condition displays exactly one fixed point $(a, -a + a^3/3)$. A linear stability analysis shows immediately that the fixed point is stable for $\mid a \mid > 1$, else unstable. As a

consequence there will be a stable limit cycle for $\mid a \mid < 1$, because there are no other fixed points and the Poincaré-Bendixson theorem applies. The results of the stability analysis are illustrated in figure 4 by means of a bifurcation diagram. The Excitator undergoes a supercritical Hopf-bifurcation at $\mid a \mid = 1$.

FIGURE FOUR HERE

Note the difference to the previously discussed equilibrium point notions [Feldman, 1980a, Feldman, 1980b, Kelso, 1977, Polit & Bizzi, 1978, Polit & Bizzi, 1979]: Equilibrium point models accomplish movement control by changing the location of an unambiguous fixed point within the location of the phase plane. As a consequence, they do not describe phenomena such as limit cycle phenomena or existence of multiple stable fixed points. In this sense, the equilibrium models may be viewed as a special case of the Excitator system. Obviously, it is acknowledged that the equilibrium point models have the benefit of making the connection to the underlying biomechanical aspects of movement control.

## 2.2 Trajectory formation in phase space: Experiment and Computation

The set of variables $x$ and $y$ provides a complete description of the dynamics of a two-dimensional excitable system. Here we use a convention most often used in the context of excitable systems [Murray, 1993, Strogatz, 1994]. This convention separates the time scales present in the dynamics, that is a fast time scale on the order $1/\tau$ associated with the $x$ variable, and a slow time scale on the order of $\tau$ associated with the variable $y$. This clear time scale separation enables us to formulate an unambiguous criterion for the separatrix, that is sufficiently fast horizontal flow away from the separatix with $\tau \gg 1$. The fixed points are obtained from the intersections of the nullclines and may be located anywhere in phase space. On the other hand, it is experimental practice to identify the second variable with the effector velocity, $y = \dot{x} = \partial_t x$. As a consequence, all fixed points are located along the horizontal x-axis. From equation (3), it is evident though that the second variable $y$ is not the effector velocity $\dot{x}$, but rather a nonlinear function of $x$ and $\dot{x}$, that is $y = \dot{x}/\tau - x + g_1(x)$. To perform a comparison between experimental and theoretical results, we have to identify a mapping between the two coordinate systems used in experiment and theory. In particular, we map the theoretical set of variables $x, y$ onto a new set of variables, $u, v$. The new set of variables is required to satisfy the condition $v = \dot{u}$. If the

mapping is a homeomorphism, the dynamics will remain the same in both coordinate systems, that is the topology of the phase flow is not altered by the mapping. In general, $x, y$ will be used for discussing the intrinsic dynamics of the Excitator in equation (3), and $u, v$ will be used for comparison with the experimental system.

We seek a mapping $h_1(x), h_2(x, y)$ such that

$$\begin{aligned} u &= h_1(x) = x \\ v &= h_2(x, y) \end{aligned} \tag{8}$$

where the new variables $u, v$ satisfy with equation (3)

$$\dot{u} = v = h_2(x, y) = (\partial_x h_1)\dot{x} = (x + y - g_1(x))\tau \qquad \text{and} \qquad \partial_x h_1 = 1 \tag{9}$$

Here $h_1$ and $h_2$ are differentiable and smooth over $x, y$ and hence will not alter the topology of the phase flow in the new coordinates $u, v$. Then the mapping from $(x, y)$ to $(u, v)$ coordinates and its inverse are given by

$$\begin{aligned} u &= x & \qquad x &= u \\ v &= (x + y - g_1(x))\tau & \qquad y &= v/\tau - u + g_1(u) \end{aligned} \tag{10}$$

The dynamics of $u, v$ may be readily written as

$$\begin{aligned} \dot{u} &= v \\ \dot{v} &= (\partial_x h_2)\,\dot{x} + (\partial_y h_2)\,\dot{y} \\ &= (1 - \underbrace{\partial_x g_1(x)\mid_{x=u}}_{\gamma_1(u)})\tau v - u - g_2(u, v) + a + I \end{aligned} \tag{11}$$

where $g_2(u, v) = g_2(u, y(u, v))$. It is fully equivalent to either solve equation (3) and then map $x, y$ onto $u, v$, or, alternatively, perform the numerical solution directly in equation (11). The specific realization of the Excitator given in equation (7) reads in $u$-$v$-coordinates as follows

$$\begin{aligned} \dot{u} &= v \\ \dot{v} &= (1 - u^2)\tau v - u - b(v/\tau - u + 1/3u^3) + a + I \end{aligned} \tag{12}$$

It is evident that the time scales of evolution are mixed in equation (12), whereas they are unmixed in equation (7).

### 2.2.1 Methods

We present briefly experimental data whose primary purpose here is to illustrate characteristic features of phase plane trajectories; its secondary purpose is to identify space and time scales

which will allow us to identify parameters in specific realizations of Excitator models (see below). Ten right handed (self-reported) male subjects took part in this experiment. All procedures were cleared by the local Human Subjects Committee and participants signed consent forms before taking part in the experiment. Participants placed the index finger of their dominant hand in a custom built manipulandum which restricted motion of the metacarpophalangeal joint to a single plane (see [Kelso & Holt, 1980] for more details about the apparatus). Unnecessary vertical and horizontal movements were restricted by a padding placed against the sides of the hand. An angle calibrated potentiometer measured the position of the index finger. Finger movement was sampled at 128Hz using an ODAU analog-digital converter connected to an Optotrak 3010 system. The external metronome, consisting of a sequence of beeps, was sent to the ODAU unit and a pair of headphones. Three experimental conditions were tested, the bistable condition (I), in which two fixed points exist, the monostable condition exhibiting only one fixed point (II) and the limit cycle condition (III). In the first two conditions, subjects were exposed to a sequence of auditory stimuli of 30ms duration and variable inter-stimulus interval (4000ms±1000ms). The subjects were instructed to react to the stimuli as quickly as possible. In condition (I), the subjects' task was to alternate between the execution of flexion and extension. In condition (II), the subjects' task was to perform a complete flexion-extension cycle and return to the initial starting point. In the last condition (III), periodic stimuli of 30ms duration were presented with an inter-stimulus interval of 1000ms. The subjects' task was to perform continuous periodic movements, coinciding peak flexion with stimulus onset.

For the computational implementation of all simulations in section 2, we choose the following specific realization of the Excitator system:

$$\begin{aligned} \dot{x} &= (x + y - (\tfrac{1}{3}x^3 + \tfrac{1}{5}x^5))\tau \\ \dot{y} &= -(x - a + by - I)/\tau \end{aligned} \tag{13}$$

with $\tau = 1$, $g_1(x) = (1/3)x^3 + (1/5)x^5$ and $g_2(x, y) = by$. The function $g_1(x)$ has been obtained from a fit of the nullcline $y = -x + g_1(x) = -x + (c_1/3)x^3 + (c_2/5)x^5$ to the experimental data in the neighborhood of the two fixed points of the bistable condition (I). The data set of a single characteristic subject was used for the parameter fit. The other conditions (II) and (III) (monostable and limit cycle) and data sets of other subjects provided similar results. The parameters $c_1 \approx c_2 \approx 1$ have been determined as to minimize the square error of the curvature of the stable manifolds, but also to provide computationally stable solutions for all task conditions (I)-(III) discussed in the current section 2. The task conditions are implemented in the term

$-a + g_2(x, y) = -a + by$ with $a, b$ varying between 0 and 2. The parameters $a$ and $b$ have been chosen to mimic the location of the fixed points in the experimental data set of the corresponding task condition. Input strength was $I = 1$ for the on-periods of the stimuli, $I = 0$ else. For the monostable condition, the input $I$ is defined to be positive for each stimulus. For the bistable condition, the sign of $I$ alternates between plus and minus. For the limit cycle condition, no input is provided, that is $I = 0$ throughout. The duration of the rectangular stimulus $I$ was one computational time unit. All simulations are performed using a fourth-order Runge-Kutta method. We also added Gaussian white noise $\xi(t)$ to the evolution equations , where

$$< \xi(t) >= 0 \qquad < \xi(t)\xi(\tau) >= Q^2\delta(t - \tau) \qquad Q = 0.01 \tag{14}$$

The triangular brackets denote time averages. We estimate the relation between the computational units and the corresponding physical units in m and sec. One computational space unit corresponds to 2cm, estimated from the radius of the limit cycle in phase space and put in correspondence with average experimental limit cycle data. This estimate also provides a good comparison between experiment and theory for the distance of the positions of the two fixed points in the bistable condition. The time unit estimate is based on the choice for the computational angular eigenfrequency $\omega = 2\pi f = 1/T = 1$ of the Excitators (see equation (12)), where $f$ is the frequency and $T$ the period of a cycle. Experimentally, preferred finger movement frequencies range from around 1.1 Hz to 3 Hz following instructions to move the finger at a comfortable pace and through a comfortable range of motion [Fink, 2002]. If we identify the preferred frequency with the eigenfrequency and estimate it as 2Hz, then one computational time unit will correspond to 80ms, or equivalently 12.5 computational time units will correspond to 1s. In the following, all theoretical predictions will be based on these estimates.

### 2.2.2 Results

We compare representative examples of time series and phase space trajectories of experimental and simulated data. The first condition is the "bistable" condition, in which a subject has to move the index finger from a position A to a position B coincident with a metronome beat. Figure 5 displays both data, experimental (left column) and simulated (right column). In the top panel, the time series of the end-effectors are shown for a few repetitions, together with the corresponding stimulus sequence. Below the phase space trajectories are plotted in $u$-$v$-coordinates (middle panel) and x-y-coordinates (bottom panel). More repetitions have been

plotted in the bottom panel than in the top panel for reasons of clarity. In both data sets, the fixed points are identified on the horizontal axis ($v = 0$) as clustering points. Note that both time series, experimental and simulated, display an overshoot when approaching the fixed point and stabilizing there. The overshoot corresponds to the movement along the return manifold discussed earlier in section 2.1. In the u-v-system (middle panel), this motion evolves along $v = 0$ by construction, whereas in the x-y-system (lower panel) the motion follows a concave curve leading to the fixed points. The mapping from u-v-coordinates to x-y-coordinates is defined by equation (10) with $\tau = 1$ and $g_1(x) = x^3/3$. In the following we will use the u-v-coordinates which may be identified with the commonly used variables position and velocity.

FIGURE FIVE HERE

The monostable condition displays one fixed point and displays a flexion-extension cycle when the fixed point is destabilized. The experimental data (left column) and simulated data (right column) are plotted in figure 6 using $u, v$-coordinates. The phase space trajectories display the fixed point on the right side of the trajectories as clear clustering points. Two of the movement cycles are plotted in the top panel. Here we note again the overshoot occurring after the execution of a flexion-extension cycle.

FIGURE SIX HERE

The overshoot and the slow fall-off towards the rest state correspond to the motion along the return manifold. The arrows in figure 6 point towards the attractive manifolds around $v = 0$. In analogy to refractory times of neurons [FitzHugh, 1961, Hodgkin & Huxley, 1952, Hindmarsh & Rose, 1982], the return phase of the movement cycle along the manifold corresponds to the refractory part of the dynamics, in which the system is more difficult to excite, and lasts until the fixed point is reached. Using the parameter identification in section 2.2.1 we estimate the movement time to be on the order of 400ms, defined from movement onset to the maximum value of extension (that is maximum positive $u$). At this latter point, the return phase of the movement cycle starts and also lasts for about 400ms in both, experimental and theoretical, data sets. However, the movement onset of the theoretical data is instantaneous at stimulus onset. The experimental data set shows the well-known delay between stimulus and movement onset which is sensory-modality dependent and is attributed to perceptual processes [Hackley & Valle-Inclán, 1998].

The experimental data (left column) and simulated data (right column) of the limit cycle condition are displayed in figure 7 in $u, v$-coordinates. The simulated trajectories appear to be more symmetric than the experimental trajectories with respect to point symmetry. Both data sets show structures that are reminiscent of the return manifolds in the neighborhood of $\mid u \mid \approx 1$, such that the deviations from the circular structure of the trajectories are more pronounced in these regions and a higher clustering of data points occurs.

FIGURE SEVEN HERE

## 3 Coupled dynamics of two Excitators

The phenomenon of in-phase and anti-phase behavior of two coupled oscillating systems is omnipresent in nature. It has received particular attention in movement science (see [Kelso, 1995, Jirsa & Kelso, 2004] for reviews), because of its simplistic nature, that is the reduction of its degrees of freedom: By forcing the effectors of the human movement system onto limit cycles, which is typically done by providing adequate task conditions, the phases of the effectors become the collective variables carrying the relevant movement information. Kelso provides a general discussion of the dynamics observable in a system described by a phase equation [Kelso, 2002]. In particular, he points out that there are coexisting integrative (converging) and segregative (diverging) tendencies in the proximity of fixed points. Kuramoto has shown that any two weakly coupled oscillators, whose limit cycle properties are preserved despite the coupling, may be reduced to a system of coupled phase equations [Kuramoto, 1984]. The stationary solutions of the phases are always the in-phase and anti-phase solutions. The stability of these solutions is determined by the details of the coupling. The constraint of limit cycle oscillators enabled Kuramoto to draw conclusions about a variety of oscillators. Here we drop this constraint of limit cycle behavior and allow arbitrary trajectories in a two-dimensional phase space, but constrain the nature of the coupling instead. Sigmoidal nonlinearities represent the most natural form of coupling in biological systems for the following reason: A population of cells without any afferent input displays only background rest activity. When the input to the cell population is increased, there is typically an initial linear increase of cell activity. At some point the cell population will reach its maximal activity possible and the response function saturates resulting in a sigmoidal response curve. Multi-modal response curves for increasing input, such that the

response of the cell population decreases and increases again, will be unlikely if they are borne by individual cell properties, since these are subject to averaging out in a cell population. However, non-monotonic behavior of neuronal firing rates has also been observed for large input to the neuron reflecting properties of fatigue and adaptation [Freeman, 1992]. In the movement sciences the HKB-coupling [Haken et al., 1985] has been successful in understanding a number of coordination phenomena on the limit cycle. This coupling function exists of a linear polynomial with a positive coefficient and a cubic polynomial with a negative coefficient. The sign and magnitude of the coefficients are determined by the stability properties observed in bimanual rhythmic coordination behavior [Haken et al., 1985, Schöner et al., 1986]. It turns out that these coefficients are the same as for the low order approximation of the sigmoid function [ Jirsa, Fuchs, & Kelso, 1998], suggesting an interpretation of the HKB coupling as a truncated sigmoid function. If the latter is true, then the well-known dependence of the neural response functions on fatigue and attention [Freeman, 1992] may be transferred to the HKB-coupling and to the movement sciences. In the following we assume a sigmoidal coupling $S$ between two Excitator units and discuss the effects of the coupling on a variety of movement types, including rhythmic and discrete movements produced by the Excitators. Whenever appropriate, we note the effects of the truncation resulting from the HKB-coupling.

As a starting point we choose two Excitators described by the two sets of variables $u_1, v_1$ and $u_2, v_2$ with the intrinsic dynamics given by equation (11). We will keep the analytical discussion more general in the sense that our following results will be valid also for intrinsic dynamics other than the Excitators. When appropriate, we will note that the results are specific for Excitators. The sigmoidal coupling $S$ as a function of $u_i, v_i$ $i = 1, 2$ is well known to represent effects of synaptic coupling of cell populations. The coupled system of two Excitators then reads

$$\begin{aligned} \dot{u}_1 &= v_1 \\ \dot{v}_1 &= -u_1 + f_1(u_1, v_1) - \partial_t S(u_1 - u_2) \\ \dot{u}_2 &= v_2 \\ \dot{v}_2 &= -u_2 + f_2(u_2, v_2) - \partial_t S(u_2 - u_1) \end{aligned} \tag{15}$$

where $f_1$ and $f_2$ denote the intrinsic dynamics of the dynamic systems involved, e.g. an Excitator dynamics. For the time being we wish to keep the specific realization of the intrinsic dynamics open. The HKB-coupling is obtained as a truncation of the expansion of the sigmoid after its second term

$$\partial_t S(u_1 - u_2) = (\dot{u}_1 - \dot{u}_2)\partial_u S(u) = (v_1 - v_2)(\alpha + \beta(u_1 - u_2)^2 + \ldots) \approx (v_1 - v_2)(\alpha + \beta(u_1 - u_2)^2) \tag{16}$$

with $\alpha, \beta$ as constant parameters. To investigate the behavior of the Excitators with respect to each other, we study the evolution of their relative distance in phase space. The Euclidean distance of two Excitators in phase space is given by $d = \sqrt{(u_1 - u_2)^2 + (v_1 - v_2)^2}$ and it evolves in time as

$$\begin{aligned} \partial_t d &= (v_1 - v_2)[(u_1 - u_2) + (\dot{v}_1 - \dot{v}_2)]/d \\ &= (v_1 - v_2)/d[\underbrace{f_1(u_1, v_1) - f_2(u_2, v_2)}_{\Delta} - \partial_t S(u_1 - u_2) + \partial_t S(u_2 - u_1)] \\ &= (v_1 - v_2)/d \times \Delta - 2\underbrace{(v_1 - v_2)^2/d}_{>0} \times \underbrace{\partial_u S(u_1 - u_2)}_{<0 \text{ or } >0} \end{aligned} \tag{17}$$

The behavior of the trajectories in phase space is then given by

$$\begin{aligned} \text{convergence} &\longleftrightarrow \partial_t d < 0 \\ \text{divergence} &\longleftrightarrow \partial_t d > 0 \end{aligned} \tag{18}$$

Let us assume for a moment that the difference in the individual dynamics is $\Delta = 0$. Then convergence is obtained if and only if

$$\text{convergence}: \quad \partial_t d < 0 \qquad \longleftrightarrow \qquad \partial_u S(u_1 - u_2) > 0 \tag{19}$$

which is always satisfied for a uni-modal sigmoid function. Hence, two sufficiently similar trajectories will always converge. In contrast, the partial derivative of the truncated sigmoidal function, $\partial_u S(u_1 - u_2) \approx \alpha + \beta(u_1 - u_2)^2$, allows also for divergence, that is

$$\text{convergence}: \quad \partial_t d < 0 \qquad \longleftrightarrow \qquad \alpha + \beta(u_1 - u_2)^2 > 0 \tag{20}$$

and

$$\text{divergence}: \qquad \partial_t d > 0 \qquad \longleftrightarrow \qquad \alpha + \beta(u_1 - u_2)^2 < 0 \tag{21}$$

FIGURE EIGHT HERE

The conditions in equations (20) and (21) contain the special case of the coupled limit cycle oscillators discussed in [Haken et al., 1985]. When constraining the dynamics of two oscillators to a one-dimensional closed loop in phase space, the limit cycle, then the greatest distance between these two oscillators becomes half of the length of the closed loop, which is identical to anti-phase motion and is stable as long as the condition in equation (21) is satisfied. This is illustrated qualitatively in figure 9. As the amplitudes $u_1, u_2$ of the oscillators decrease with increasing movement frequency [Haken et al., 1985, Kay et al., 1987], the divergence condition

cannot be satisfied anymore and the oscillators bifurcate into in-phase motion, which is the smallest distance between two limit cycle oscillators and is always stable for $\alpha > 0$.

FIGURE NINE HERE

Another special case of the equation (17) has been first observed numerically by Schöner [Schöner , 1990] for discrete movement trajectories. Here the simulation of two Gonzalez-Piro oscillators [Gonzalez & Piro, 1987], which were coupled by means of the HKB coupling, revealed the tendency to synchronize two movements when the movement onsets were sufficiently close. Otherwise the tendency to sequentialize the movements was observed. We now may be more specific. It actually is not the movement onset times, but rather the difference in positions between the oscillators in equations (20), (21), which provides the critical value for convergence/divergence of trajectories.

The general case, $\Delta \neq 0$, introduces considerations on symmetry and similarity between the two movement trajectories. When two identical systems display the same trajectory formation, stationary or transient, then the resulting dynamics is determined solely by their mutual coupling and the earlier special case, $\Delta = 0$, is present. If the symmetry between the systems is broken, e.g. they have slightly different eigenfrequencies, then this will be reflected in $\Delta$ (for the special case of weakly coupled limit cycle oscillators see [Kuramoto, 1984, Kelso et al., 1990]). Equivalently, if two identical systems take different paths in phase space, e.g. slightly different positions, this will also be reflected in $\Delta$. We wish to identify now the intrinsic dynamics of the two coupled systems with the Excitators in equations (11) and write for the difference $\Delta$ of the intrinsic Excitator dynamics

$$\Delta = a_1 - a_2 + (1 - \gamma_1(u_1))\tau v_1 - (1 - \gamma_1(u_2))\tau v_2 - g_2(u_1, v_1) + g_2(u_2, v_2) \tag{22}$$

where $\gamma_1(u_i) = \partial_x g_1(x) \mid_{x=u_i}$. For a moment, we wish to refer back to the Excitator system in equation (3) in the $x, y$-coordinates and use the convenient property of unmixing of the time scales in this coordinate system. In particular, there are two sequentially occurring separate time scales, that is a fast horizontal flow and a slow dynamics around the outer branches (that is $x > a$) of the nullcline $y = -x + g_1(x)$ (see e.g. [Campbell & Wang, 1998] for a technical review). Using equation (10), the slow manifold reads $v = 0$ in $(u, v)$-coordinates. Most of the time during a stationary or transient dynamics will be spent on this slow manifold in the phase space. Hence we can make the following argument: Because $\gamma_1(u)$ is symmetric, that

is $\gamma_1(-u) = \gamma_1(u)$ for $u = u_1, u_2$, there will be a lower bound for the expression $\gamma_1$ for both Excitators and both slow manifolds such as

$$\gamma_1(u) \geq \gamma_1(a), \quad u = u_1, u_2;\ a = \max(a_1, a_2) \tag{23}$$

This argument may be made for $\gamma_1(u_1), \gamma_1(u_2)$ because of its symmetry property, but not for the coupling $S(u_1 - u_2)$, which depends on the difference of $u_1, u_2$. Then $\Delta$ may be approximated (for sufficiently large $\tau$ and thus time scale separation) as

$$\Delta \approx a_1 - a_2 + (1 - \gamma_1(a_1))\tau(v_1 - v_2) \tag{24}$$

and the time evolution of the trajectories' distance reads

$$\partial_t d \;=\; (v_1 - v_2)/d \times (a_1 - a_2) - 2\underbrace{(v_1 - v_2)^2/d}_{>0} \times \underbrace{((\gamma_1(a_1)) - 1)\tau/2 + \partial_u S(u_1 - u_2)}_{<0 \text{ or } >0} \tag{25}$$

In particular, if the fixed points $(u_i, v_i) = (a_i, 0),\ i = 1, 2$ are stable and the symmetry breaking is small, $\mid a_1 - a_2 \mid \ll 1$, then equation (25) is a first good approximation of the time evolution of the distance of two nearby trajectories. The sign of the last term will be the relevant criterion deciding about convergence or divergence. The critical trajectory distance is then given by

$$d_c = \mid u_1 - u_2 \mid = \sqrt{\frac{[\gamma_1(a_1) - 1]\tau/2 + \alpha}{-\beta}} \tag{26}$$

If $d > d_c$, then the trajectories will diverge, else they will converge. In the following we will test these predictions numerically.

The following simulations of the coupled Excitators are based on the Excitator model in equation (13) and its space and time scales as established in section 2.2.1. The coupling is the HKB-coupling as determined in [Haken et al., 1985, Schöner et al., 1986] and discussed in the context of neural response functions in [Jirsa et al., 1998]. The explicit equations read in $(u, v)$-coordinates:

$$\begin{aligned}
\dot{u}_1 &= v_1 \\
\dot{v}_1 &= (1 - u_1^2 - u_1^4)\tau v_1 - u_1 + a_1 + I_1 - (v_1 - v_2)(\alpha + \beta(u_1 - u_2)^2) \\
\dot{u}_2 &= v_2 \\
\dot{v}_2 &= (1 - u_2^2 - u_2^4)\tau v_2 - u_2 + a_2 + I_2 - (v_2 - v_1)(\alpha + \beta(u_1 - u_2)^2)
\end{aligned} \tag{27}$$

The parameters are $a_1 = a_2 = 1.05$, $\tau = 3$, $\alpha = 0.2$, $\beta = -0.2$. The choice of parameters resembles the monostable task condition with a single fixed point. The amplitude of the input

stimulus is $I = -3.5$ and its duration is 80msec. As described in section 2.2.1, a fourth order Runge-Kutta method including a linear noise term is used for the numerical implementation. With these parameters, the critical trajectory distance in equation (26) is estimated to be $d_c = 3.3$ in computational space units, which corresponds to about 6.5cm, and thus suggests the spatial scale of the convergence/divergence phenomena to be of the order of magnitude which is experimentally observable. Figure 10 shows the numerical simulations of the dynamics of two coupled Excitators (solid lines) following two input signals with a short inter-stimulus interval (ISI) of 80msec. Here the first stimulus is delivered to the first Excitator unit, and the second stimulus to the second Excitator unit. A comparison is made to the uncoupled trajectories (dotted lines). It can be clearly seen that the first system is delayed due to the coupling in order to achieve a more simultaneous coordination dynamics, that is convergence. Both couplings, the fully sigmoidal and its truncated form, the HKB-coupling, accomplish this phenomenon.

FIGURE TEN HERE

Figure 11 shows the same situation as before, only the ISI of the two consecutive stimuli has been increased to 160msec. Again the trajectories converge initially, such that the first Excitator is delayed as in the previous case. But upon reaching a critical value of the trajectory distance, $d = \mid x_1 - x_2 \mid \approx 2.6$ computational space units around time point 1000msec, the trajectories start diverging. As a consequence, both Excitators are delayed with respect to the uncoupled system and also with respect to each other. Such acceleration phenomena have been observed experimentally [Kelso et al., 1979, Kelso et al., 1983]. The divergence cannot be observed when using a sigmoidal coupling, because the divergence condition in equation (18) cannot be satisfied.

FIGURE ELEVEN HERE

To illustrate the quantitative degree of convergence and divergence we calculate the mean time delay between coupled and uncoupled Excitator units. Figure 12 displays the mean time difference (upper graphs) and its variance (lower graphs) as a function of the ISI. As a measure we choose the time difference between the positions of two Excitators when they cross $x = 1$ after a flexion-extension cycle (just before they enter the return phase). The mean time difference was computed from 11 trials as a function of the ISI. With a dynamics as defined in equation (27), the coupled Excitator units show convergence times of coordinated action up to 50msec for ISIs from 0 to 130ms. For ISIs greater than 130msec, the coupled system displays divergence,

though to a smaller extent (up to 30msec). For ISIs between 100msec and 150msec, the variance of the time difference of the coupled system (solid line) is greatly enhanced. Since the variance of the uncoupled system (dashed line) is also enhanced in a similar range of ISIs, it is implied that an increased sensitivity of the intrinsic Excitator dynamics rather than the coupling is the cause of the increased variance.

FIGURE TWELVE HERE

# 4 Conclusions

What have we accomplished by developing a "minimal model" that we have named here as the "Excitator"? First, the Excitator summarizes the mathematical properties, that a two-dimensional dynamic system based on ordinary differential equations must have to produce a set of behaviors, the most striking ones being discrete and rhythmic movements, and false starts. Among other models, the HKB-model [Haken et al., 1985], Schöner's model [Schöner , 1990] and many neuronal models, such as the FitzHugh-Nagumo system [FitzHugh, 1961], the Hodgkin-Huxley equations [Hodgkin & Huxley, 1952] and the Hindmarsh-Rose oscillator [Hindmarsh & Rose, 1982], are specific realizations of the Excitator for special parameter settings, in the sense that all of the prior models produce only a subset of behaviors. The virtue of the current description is its generality which is based on the discussion of topological elements of the flow in phase space such as separatrices and stability of fixed points. The existence of these structural features is invariant under homeomorphisms (see the Hartmann-Grobmann theorem, e.g. [Guckenheimer & Holmes, 1983, Perko, 1991]) and arguments on the actual implementation of the dynamics of the system become superfluous [Peper & Beek, 1998]. However, admittedly, the specifics of implementation become relevant when addressing the dynamics and its underlying neuronal substrate, because here the material realization will provide us with additional information on the shape of the mathematical terms present in the Excitator. As an example, neuronal response functions are typically understood to be sigmoidal and their slope and height vary with the degree of attention [Freeman, 1992]. Such identification of the sigmoidal response function with the Excitator couplings provides us with an entry point to attentional, or more generally, cognitive influences on the behavioral system and constrains the vast space of possible modelling. We propose a specific realization of the Excitator which is not unique, but allows for

explicit quantitative predictions. For example, we predict the existence of an attractive manifold in the phase space (the return phase after the overshoot) along which the system evolves for a duration on the order of 400msec. The manifold constrains the flow in the phase space to a limited region and hence constrains the movement dynamics. The motion along the manifold has refractory properties, such that perturbations or additional stimuli will excite the movement system less effectively until the final rest state is reached. Further, we postulated the existence of a separatrix in phase space and predict that the probability of the occurence of false starts increases with decreasing distance to the separatrix. More specifically, shifts of the location of the equilibrium point in phase space towards the separatrix are predicted to cause more false starts. The probability of the occurrence of a false start will be a function of three factors: 1. the distance between the fixed point and the separatrix; 2. the strength of the flow away from the separatrix; 3. the noise strength. All three components are experimentally accessible and allow the calculation of a mean escape time which is directly related to the probability of the occurrence of a false start (see [Schöner et al., 1986, Fuchs & Jirsa, 2000] for stochastic treatments of rhythmic movements). An experimental demonstration of the existence of a separatrix (the backbone of the Excitator) involves to show a correlation between the probability of a false start and the three components above. Finally, a general discussion of coupled Excitators leads us to the prediction that the timing of coordinated multilimb movements primarily depends on the difference in the positions of the effectors, a phenomenon first noted in slightly different form [Schöner , 1990]. Our analysis shows that for inter-stimulus intervals of less than 130msec, two movements tend to be executed synchronously; conversely, for inter-stimulus intervals of more than 130msec, two movements tend to be executed sequentially. Both effects are on the order of 30msec to 50msec.

## 5 Acknowledgements

The help of Felix Almonte and Collins Assisi during movement data collection is much appreciated. We thank Ajay Pillai for help during the final editorial process and two anonymous reviewers who provided very helpful comments. This work was supported by DARPA grant NBCH1020010, NIMH Grants MH42900 and MH01386.

# A Appendix

Here we shall derive the constraints given in equation (4) for the system defined in equation (3).

## A.1 Existence of separatrix

The horizontal flow shall be given by $\dot{x} = x + y - g_1(x)$. In a neighborhood $U$ of the origin $(x, y) = (0, 0)$, the smooth function $g_1(x)$ shall have the following Taylor expansion

$$g_1(x) = \frac{1}{2!}\partial_x^2 g_1(0)x^2 + \frac{1}{3!}\partial_x^3 g_1(0)x^3 + \dots \tag{28}$$

which means $g_1(0) = 0$ and $\partial_x g_1(0) = 0$. Then the horizontal flow in $U$ is given by $y = -x$ sufficiently close to the origin and is repelling.

## A.2 Existence of fixed point $(x_0, y_0)$

There will be n fixed points, if and only if the nullclines of equation (3) intersect in n points in the phase space.

## A.3 Stability of fixed point $(x_0, y_0)$

The stability of the fixed point is determined by the eigenvalues of the Jacobian $L$ defined as

$$L = \begin{pmatrix} (1 - \partial_x g_1)\tau & \tau \\ -(1 + \partial_x g_2)/\tau & -\partial_y g_2/\tau \end{pmatrix} \tag{29}$$

where the partial derivatives are to be evaluated at $(x_0, y_0)$. The eigenvalues are obtained from the characteristic polynomial $\det(L - \lambda I) = 0$, with $I$ as the identity matrix, and read

$$\lambda = \frac{1}{2}(-\partial_y g_2/\tau - \tau(\partial_x g_1 - 1) \pm \sqrt{\text{root}}) \tag{30}$$

with

$$\text{root} = (\partial_y g_2/\tau + \tau(\partial_x g_1 - 1))^2 - 4(\partial_y g_2(\partial_x g_1 - 1) + 1 + \partial_x g_2) \tag{31}$$

To simplify this ugly term we use the sequential time scale hierarchy present in relaxation oscillators, that is $\tau \gg 1$, neglect $\partial_y g_2/\tau$ and write

$$\lambda = \frac{1}{2}(-\tau(\partial_x g_1 - 1) \pm \sqrt{\tau^2(\partial_x g_1 - 1)^2 - 4[\partial_y g_2(\partial_x g_1 - 1) + 1 + \partial_x g_2]}) \tag{32}$$

If $\mathrm{Re}[\lambda] < 0$, then the fixed point $(x_0, y_0)$ is stable. This results in the stability conditions

$$\partial_x g_1 > 1 \qquad \text{and} \qquad \partial_y g_2(\partial_x g_1 - 1) + 1 + \partial_x g_2 > 0 \tag{33}$$

### A.4 Boundedness

The condition for sequential time scale hierarchy, $\tau \gg 1$, shall be satisfied. Then the center manifold theorem applies [Perko, 1991] and the fast variable, $x$, may be adiabatically eliminated [Haken, 1983], $\dot{x} = 0$, such that all the horizontal flow is contracted to $y = -x + g_1(x) \approx g_1(x)$, sufficiently far away from the origin. We require that the inverse of $g_1^{-1}$ exists at least locally in phase space, $x = g_1^{-1}(y)$. Then the vertical phase flow may be expressed as

$$\dot{y} = -\frac{1}{\tau}(\underbrace{g_1^{-1}(y) - a + g_2(g_1^{-1}(y), y)}_{G(y)}) \tag{34}$$

and will be directed towards the origin for large $y$, if and only if

$$G(y) = G(y \to \pm\infty) \to \pm\infty \tag{35}$$

As a consequence, if the nonlinear function $g_1(x)$ satisfies $g_1(x \to \pm\infty) \to \pm\infty$ also, then it follows that the horizontal flow is always directed towards the origin for large $x$. A slightly stronger constraint for the boundedness of horizontal and vertical flow is obtained by requiring point symmetry: $g_1(-x) \overset{x\to\pm\infty}{\longrightarrow} -g_1(x)$ and $G(-y) \overset{y\to\pm\infty}{\longrightarrow} -G(y)$.

## References

[Amari, 1977] Amari, S. (1977). Dynamics of pattern formation in lateral-inhibition type neural fields. *Biological Cybernetics*, *27*, 77-87.

[Balasubramaniam & Feldman, 2004] Balasubramaniam, R., Feldman, A.G. (2004). Guiding movements without redundancy problems. In Jirsa, V.K. & Kelso, J.A.S. (Eds.), *Coordination dynamics: Issues and trends* (pp. 155-176). New York: Springer.

[Beek et al., 2002] Beek, P.J., Peper, C.E. & Daffertshofer, A. (2002). Modeling rhythmic interlimb coordination: Beyond the Haken-Kelso-Bunz model. *Brain and Cognition*, *48 (1)*, 149-165.

[Campbell & Wang, 1998] Campbell, S.R. & Wang, D. (1998). Relaxation oscillators with time delay coupling. *Physica D*, *111 (1-4)*, 151-178.

[Collet, 1999] Collet, C. (1999). Strategic aspects of reaction time in world-class sprinters. *Perceptual and Motor Skills*, *88 (1)*, 65-75.

[Croot et al., 2000] Croot, K., Hodges, J.R., Xuereb, J. & Patterson, K. (2000). Phonological and articulatory impairment in Alzheimer's disease: A case series. *Brain and Language*, *75*, 277-309.

[Daffertshofer et al., 2004] Daffertshofer, A., Peper, C.E. & Beek, P.J., (2003). Stabilization of bimanual coordination due to active inhibition - evidence from phase transitions. submitted.

[Feldman, 1980a] Feldman, A.G. (1980). Superposition of motor programs. I. Rhythmic forearm movements in man. *Neuroscience*, *5*, 81-90.

[Feldman, 1980b] Feldman, A.G. (1980). Superposition of motor programs. II. Rapid flexion of forearm in man. *Neuroscience*, *5*, 91-95.

[Fink, 2002] Fink, P. (2002). private communication.

[FitzHugh, 1961] FitzHugh, R. (1961). Impulses and physiological states in theoretical models of nerve membrane. *Biophysical Journal*, *1*, 445-466.

[Freeman, 1992] Freeman, W.J. (1992). Tutorial on neurobiology: From single neurons to brain chaos. *International Journal of Bifurcation and Chaos*, *2*, 451-482.

[Fuchs et al., 1992] Fuchs, A., Kelso, J.A.S. & Haken, H. (1992). Phase Transitions in the Human Brain: Spatial Mode Dynamics. *International Journal of Bifurcation and Chaos*, *2*, 917-939.

[Fuchs & Jirsa, 2000] Fuchs, A. & Jirsa, V.K. (2000). The HKB Model revisited: How varying the degree of symmetry controls dynamics. *Human Movement Science 19, 4*, 425-449.

[Fuchs et al., 2000] Fuchs, A., Jirsa, V.K. & Kelso, J.A.S. (2000). Theory of the relation between human brain activity (MEG) and hand movements. *Neuroimage 11*, 359-369.

[Fuchs et al., 2000] Fuchs, A., Mayville, J.M., Cheyne, D., Weinberg, H., Deecke, L. & Kelso, J.A.S. (2000). Spatiotemporal analysis of neuromagnetic events underlying the emergence of coordinative instabilities. *Neuroimage*, *12*, 71-84.

[Gonzalez & Piro, 1987] Gonzalez, D.L. & Piro, O. (1987). Global bifurcations and phase portrait of an analytically solvable nonlinear oscillator: relaxation oscillations and saddle-node collisions. *Physical Review A*, *36* , 4402-4410.

[Grossberg et al., 1997] Grossberg, S., Pribe, C. & Cohen, M.A. (1997). Neural control of interlimb oscillations. I. Human bimanual coordination. *Biological Cybernetics*, *77*, 131-140.

[Guckenheimer & Holmes, 1983] Guckenheimer, J. & Holmes, P. (1983). *Nonlinear oscillations, dynamical systems, and bifurcations of vector fields.* New York: Springer.

[Hackley & Valle-Inclán, 1998] Hackley, S.A. & Valle-Inclán (1998). Automatic alerting does not speed late motoric processes in a reaction-time task. *Nature*, *391*, 786-788.

[Haken, 1983] Haken, H. (1983). *Synergetics. An Introduction. 3rd ed.*, Berlin, Heidelberg, New York: Springer.

[Haken et al., 1985] Haken, H., Kelso, J.A.S. & Bunz, H. (1985). A Theoretical Model of Phase transitions in Human Hand Movements. *Biological Cybernetics*, *51*, 347-356.

[Haken, 1996] Haken, H. (1996). *Principles of brain functioning.* Berlin, Heidelberg, New York: Springer.

[Haken, 2002] Haken, H. (2002). *Brain Dynamics.* Berlin, Heidelberg, New York: Springer.

[Hindmarsh & Rose, 1982] Hindmarsh, J.L. & Rose, R.M. (1982). A model of the nerve impulse using two first-order differential equations. *Nature*, *296 (5853)*, 162-164.

[Hodgkin & Huxley, 1952] Hodgkin, A.L. & Huxley, A.F. (1952). A quantitative description of membrane current and its application to conduction and excitation in nerve. *Journal of Physiology*, *117*, 500-544.

[Jirsa et al., 1994] Jirsa, V.K., Friedrich, R., Haken, H. & Kelso, J.A.S.(1994). A theoretical model of phase transitions in the human brain. *Biological Cybernetics*, *71*, 27-35.

[Jirsa et al., 1995] Jirsa, V.K., Friedrich, R. & Haken, H. (1995). Reconstruction of the spatiotemporal dynamics of a human magnetoencephalogram. *Physica D*, *89*, 100-122.

[Jirsa & Haken, 1996] Jirsa, V.K. & Haken, H. (1996). Field theory of electromagnetic brain activity. *Physical Review Letters*, *77*, 960-963.

[Jirsa & Haken, 1997] Jirsa, V.K. & Haken, H. (1997). A derivation of a macroscopic field theory of the brain from the quasi-microscopic neural dynamics. *Physica D*, *99*, 503-526.

[Jirsa et al., 1998] Jirsa V.K., Fuchs, A. & Kelso, J.A.S. (1998). Connecting cortical and behavioral dynamics: bimanual coordination. *Neural Computation*, *10*, 2019-2045.

[Jirsa & Kelso, 2000] Jirsa, V.K. & Kelso, J.A.S. (2000). Spatiotemporal pattern formation in neural systems with heterogeneous connection topologies. *Physical Review E*, *62*, 8462–8465.

[Jirsa, 2003] Jirsa, V.K. (2003). Information processing in brain and behavior displayed in large-scale topographies such as EEG and MEG. *International Journal of Bifurcation and Chaos*, (in press)

[Jirsa & Kelso, 2004] Jirsa, V.K. & Kelso, J.A.S. (2004) *Coordination dynamics: Issues and trends*. New York: Springer.

[Kay et al., 1987] Kay, P.A., Kelso, J.A.S., Saltzmann, E.L. & Schöner, G. (1987). Space-time behavior of single and bimanual rhythmical movements: data and limit cycle model. *Journal of Experimnetal Psychology*, *13*, 178-192.

[Kelso, 1977] Kelso, J.A.S. (1977). Motor control mechanisms underlying human movement reproduction. *Journal of Experimental Psychology: Human Perception and Performance*, *3*, 529-543.

[Kelso et al., 1979] Kelso, J.A.S., Southard, D. & Goodman, D. (1979). On the coordination of two-handed movements. *Journal of Experimental Psychology: Human Perception and Performance*, *5*, 229-238.

[Kelso & Holt, 1980] Kelso, J.A.S & Holt, K.G. (1980). Exploring a vibratory systems-analysis of human movement production. *Journal of Neurophysiology*, *43 (5)*, 1183-1196.

[Kelso, 1981] Kelso, J.A.S. (1981). On the oscillatory basis of movement. *Bulletin of Psychonomic Society*, *18*, 63.

[Kelso et al., 1983] Kelso, J.A.S., Putnam, C.A. & Goodman, D. (1983). On the space-time structure of human interlimb coordination. *Quarterly Journal of Experimental Psychology*, *35A*, 347-375.

[Kelso, 1984] Kelso, J.A.S. (1984). Phase transitions and critical behavior in human bimanual coordination. *American Journal of Physiology*, *15*, R1000-R1004.

[Kelso et al., 1990] Kelso, J.A.S., DelColle J.D. & Schöner G. (1990). Action-perception as a pattern formation process. In Jeannerod, M. (Eds.), *Attention and performance XIII* (136-169). Hillsdale, NJ: Erlbaum.

[Kelso et al., 1992] Kelso, J.A.S., Bressler, S.L., Buchanan, S., DeGuzman, G.C., Ding, M., Fuchs, A. & Holroyd, T. (1992). A Phase Transition in Human Brain and Behavior. *Physics Letters A*, *169*, 134-144.

[Kelso, 1995] Kelso, J.A.S (1995). *Dynamic Patterns. The Self-Organization of Brain and Behavior*. Cambridge, Massachusetts: MIT Press.

[Kelso et al., 1998] Kelso, J.A.S., Fuchs, A., Lancaster, R., Holroyd, T., Cheyne, D. & Weinberg, H. (1998). Dynamic cortical activity in the human brain reveals motor equivalence. *Nature*, *23*, 814-818.

[Kelso, 2002] Kelso, J.A.S. (2002). The complementary nature of coordination dynamics: Self-Organization and the origins of agency. *Journal of Nonlinear Phenomena in Complex Systems*, *5*, 364-371.

[Kuramoto, 1984] Kuramoto, Y. (1984). Chemical oscillations, waves, and turbulence, Berlin, Heidelberg, New York: Springer.

[Mayville et al., 2002] Mayville, J.M., Jantzen, K.J., Fuchs, A., Steinberg, F.L. & Kelso J.A.S. (2002). Cortical and subcortical networks underlying syncopated and synchronized coordination revealed using fMRI. *Human Brain Mapping*, *17*, 214-229.

[Meyer-Lindenberg et al., 2002] Meyer-Lindenberg, A., Ziemann, U., Hajak, G., Cohen, L. & Berman, K.F. (2002). Transitions between dynamical states of differing stability in the human brain. *Proceedings of the National Academy of Sciences*, *99 (17)*, 10948-10953.

[Murray, 1993] Murray, J.D. (1993). *Mathematical Biology*. Springer.

[Nagashino & Kelso, 1992] Nagashino, H. & Kelso, J.A.S. (1992). Phase transitions in oscillatory neural networks.*Science of Artificial Neural Networks, International Society for Optical Engineering*, *1710*, 278-297.

[Nunez, 1974] Nunez, P.L. (1974). The brain wave equation: A model for the EEG. *Mathematical Biosciences*, *21*, 279-297.

[Nunez, 1995] Nunez, P.L. (1995). *Neocortical dynamics and human EEG rhythms.* Oxford University Press.

[Peper & Beek, 1998] Peper, C.L.E. & Beek, P.J. (1998). Are frequency-induced transitions in rhythmic coordination mediated by a drop in amplitude? *Biological Cybernetics 79 (4)*, 291-300.

[Perko, 1991] Perko, L. (1991). *Differential equations and dynamical systems.*Berlin, Heidelberg, New York: Springer.

[Polit & Bizzi, 1978] Polit, A. & Bizzi, E. (1978). Processes controlling arm movements inmonkeys. *Science*, *201*, 1235-1237.

[Polit & Bizzi, 1979] Polit, A., & Bizzi, E. (1979). Characteristics of motor programsunderlying arm movements in monkeys. *Journal of Neurophysiology*, *42*, 183-194.

[Postma, 2000] Postma, A. (2000). Detection of errors during speech production: a review of speech monitoring models. *Cognition*, *77*, 97-131.

[Pribe et al., 1997] Pribe, C., Grossberg, S. & Cohen, M.A. (1997). Neural control of interlimb oscillations. II. Biped and quadruped gaits and bifurcations. *Biological Cybernetics*, *77*, 141-152.

[Robinson et al., 1997] Robinson, P.A., Rennie, C.J. & Wright, J.J. (1997). Propagation and stability of waves of electrical activity in the cerebral cortex. *Physical Review E*, *56*, 826.

[Schmidt & Gordon, 1977] Schmidt, R.A., & Gordon, G.B. (1977). Errors in motor responding, "rapid" corrections, and false anticipations. *Journal of Motor Behavior*, *9*, 101-111.

[Schmidt & Mc Gown, 1980] Schmidt, R.A. & Mc Gown, C. (1980). Terminal accuracy of unexpectedly loaded rapid movements. Evidence for a mass-spring mechanism in programming. *Journal of Motor Behavior*, *12*, 149-161.

[Schöner et al., 1986] Schöner, G., Haken, H., & Kelso, J.A.S. (1986). A stochastic theory of phase transitions in human hand movement. *Biological Cybernetics*, *53*, 247-257.

[Schöner , 1990] Schöner, G. (1990). A dynamic theory of coordination of discrete movement.*Biological Cybernetics*, *63*, 257-270.

[Sternad et al., 2000] Sternad, D., Dean, W.J. & Schaal, S. (2000). Interaction of rhythmic and discrete pattern generators in single-joint movements. *Human Movement Science*, *19(4)*, 627-664.

[Strogatz, 1994] Strogatz, S.H. (1994). *Nonlinear Dynamics and Chaos*. Addison-Wesley.

[Wilson & Cowan, 1972] Wilson, H.R. & Cowan, J.D. (1972). Excitatory and inhibitory interactions in localized populations of model neurons. *Biophysical Journal*, *12*, 1-24.

[Wilson & Cowan, 1973] Wilson, H.R. & Cowan, J.D. (1973). A mathematical theory of the functional dynamics of cortical and thalamic nervous tissue. *Kybernetik*, *13*, 55-80.

[Wing & Kristofferson, 1973] Wing, A.M. & Kristofferson A.B. (1973). Response delays and the timing of discrete motor responses. *Perception and Psychophysics*, *14*, 5-12.

[Wright & Liley, 1996] Wright, J.J. & Liley, D.T.J. (1996). Dynamics of the brain at global and microscopic scales: Neural networks and the EEG. *Behavioral Brain Sciences*, *19*, 285.

[Young & Freedman, 1996] Young, H.D. & Freedman, R.A. (1996). *University Physics*. Addison-Wesley

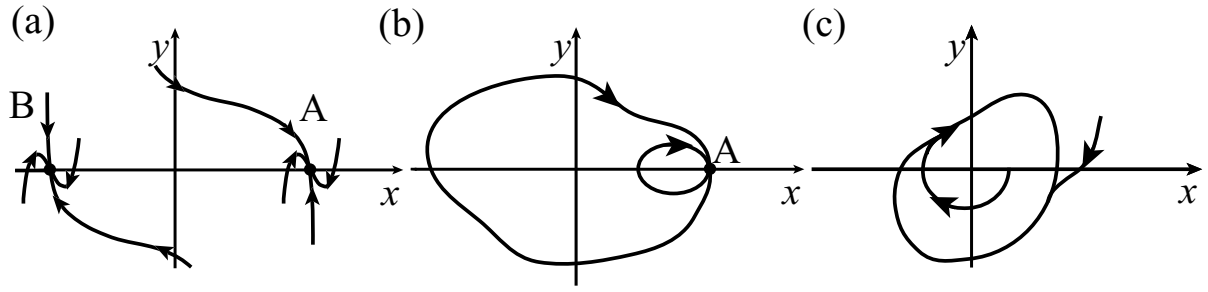


Figure 1: **Topological features of phase flow: a) two stable fixed points A and B; b) one stable fixed point A displaying either small amplitude deviations or large amplitude orbits; c) stable limit cycle.** $x$ **and** $y$ **are variables (such as position and velocity) in the two-dimensional phase space.**

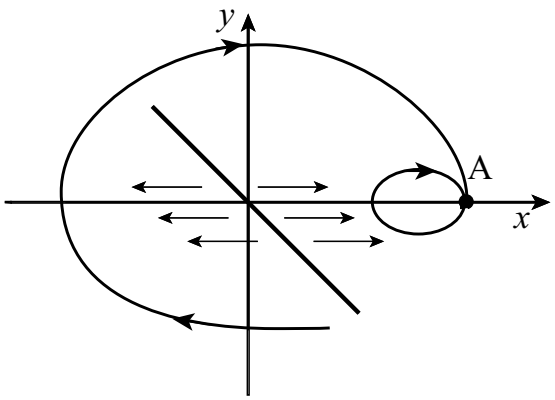


Figure 2: **A separatrix divides the phase flow locally into two separate regimes located to its left and right, thereby creating a threshold element and thus the propensity to false starts. The direction of flow is indicated by arrows.**

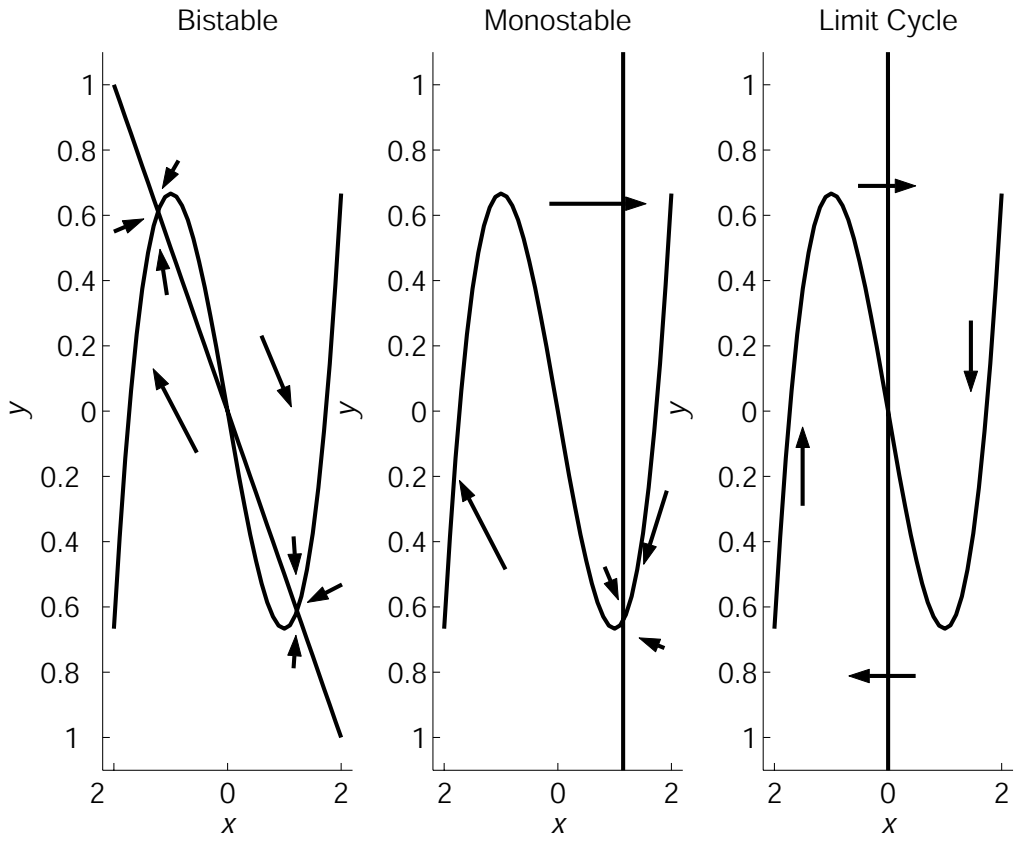


Figure 3: **The nullclines for the three conditions bistable, monostable and limit cycle, are plotted together with arrows indicating the direction of the flow in the phase space. The cubic curve is the nullcline for $\dot{x} = 0$ and remains unchanged, only the $(\dot{y} = 0)$ - nullcline is altered to define the task conditions by adjusting the flow and topology in phase space.**

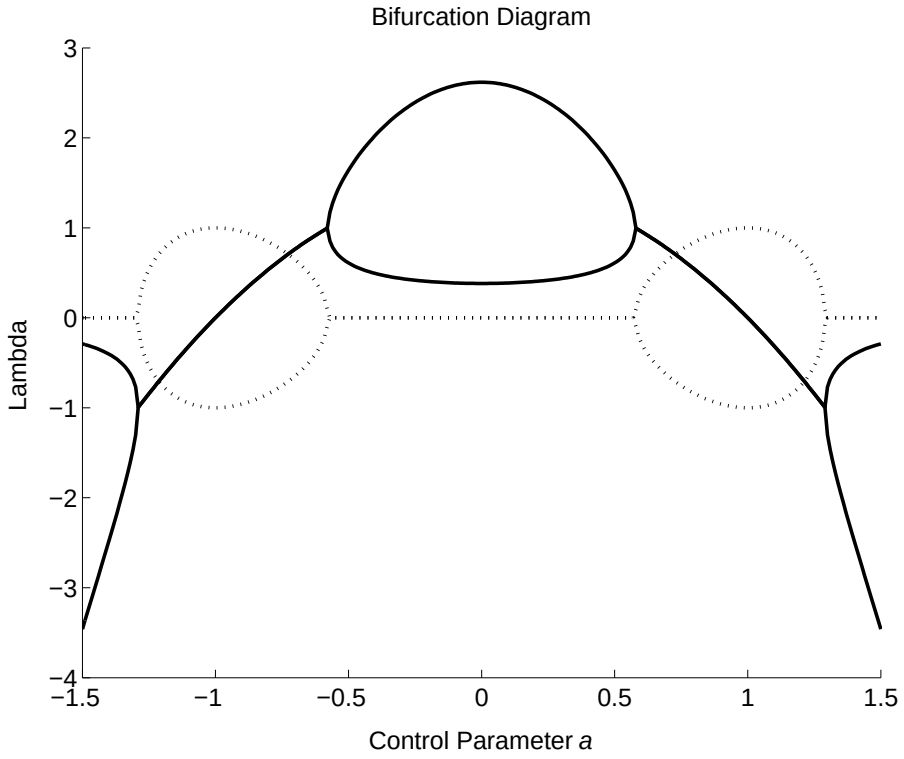


Figure 4: **The real parts (solid line) and the imaginary parts (dotted line) of the eigenvalue of the linear stability analysis around the fixed point A are plotted in this bifurcation diagram. A supercritical Hopf-bifurcation occurs at** $\mid a \mid = 1$**.**

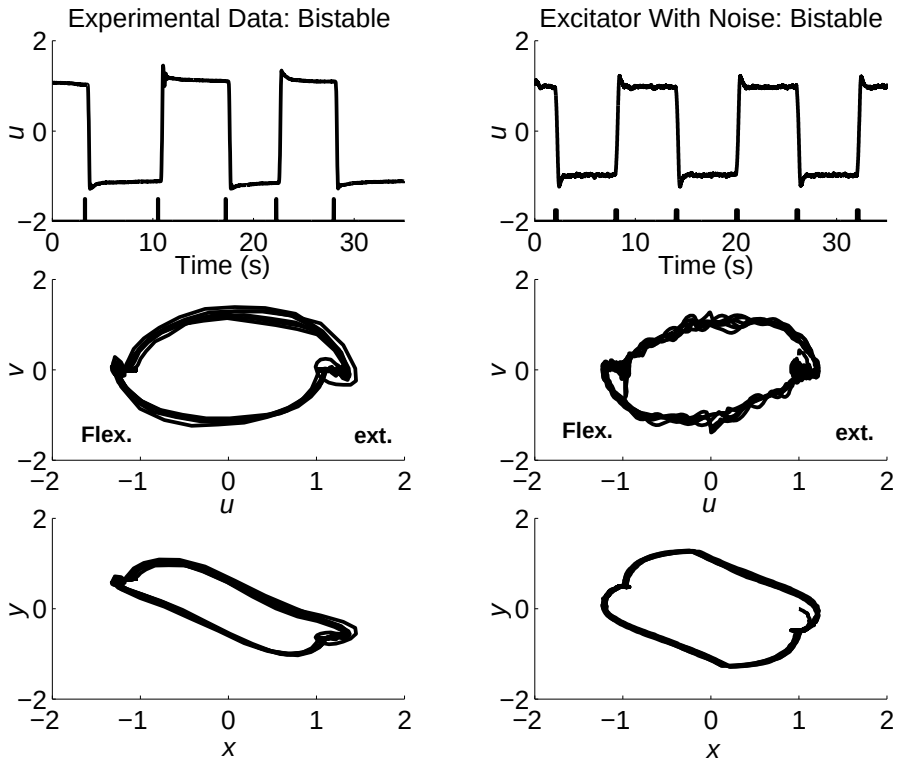


Figure 5: **Two fixed points A and B were created in phase space. The left column shows experimental data, the right column numerical simulations. The time units are in seconds, the space units are dimensionless. The phase space trajectories are represented in the u-v-coordinate system (middle panel), which ensures that the fixed points are located along the horizontal axis in phase space, as well as in the x-y-coordinate system (lower panel). The mapping given in equation (10) has been used with $\tau = 1$ and $g_1(x) = x^3/3$.**

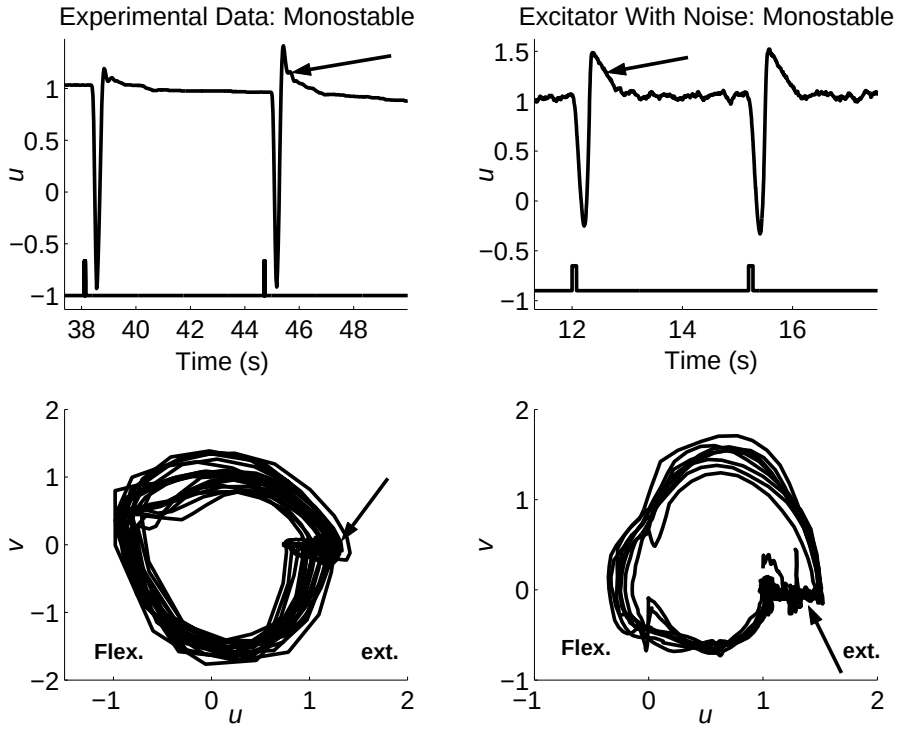


Figure 6: **One fixed point A is created in phase space. The left column shows experimental data, the right column displays the results of the numerical simulations. The time units are in seconds, the space units are dimensionless. Both data sets are represented in the u-v-coordinate system. The dynamics along the attractive return manifolds, $v \approx 0$, is indicated by arrows in the time series and the phase spaces.**

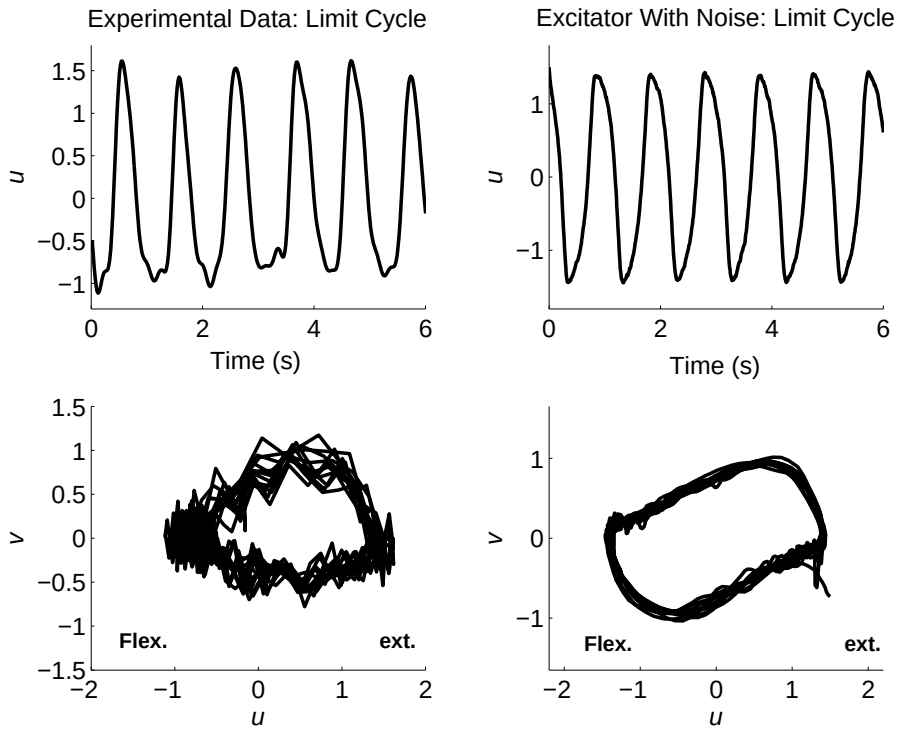


Figure 7: **A limit cycle is created in phase space. The left column shows experimental data, the right column displays the results of the numerical simulations. The time units are in seconds, the space units are dimensionless. Both data sets are represented in the u-v-coordinate system.**

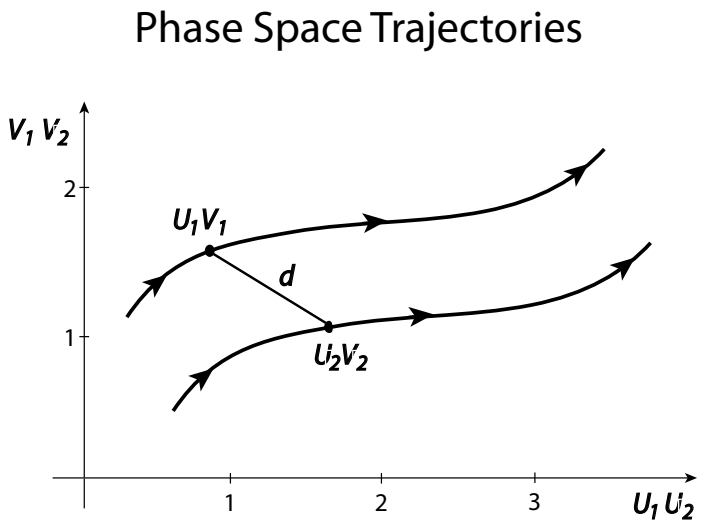


Figure 8: **Two phase space trajectories are shown. The instantaneous Euclidean distance $d(t)$ in phase space is a measure of the similarity of two on-going dynamics.**

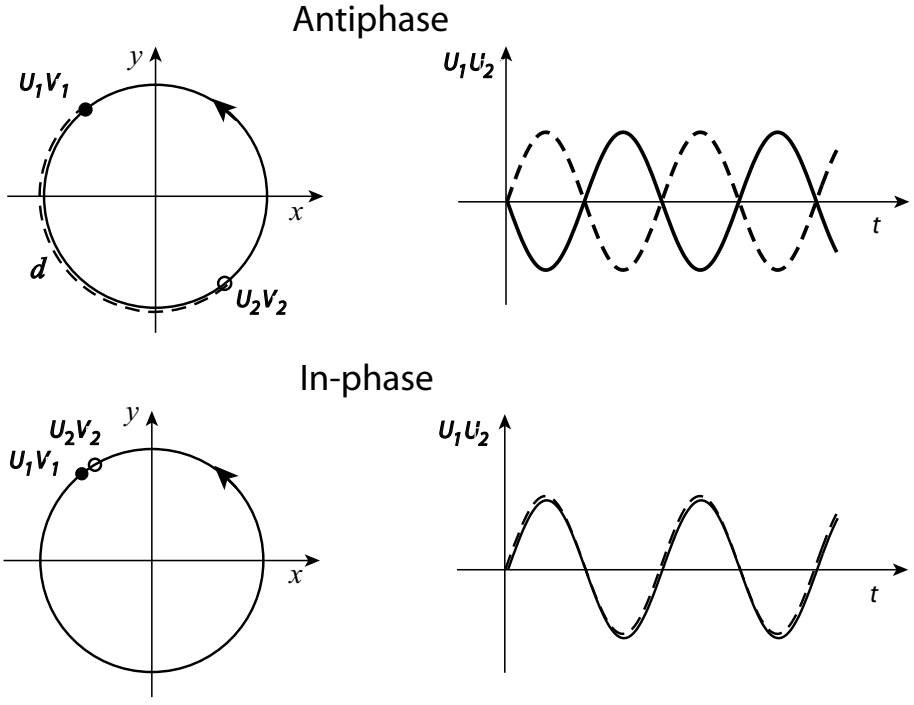


Figure 9: **The Euclidean distance d of two limit cycle oscillators is maximal for anti-phase motion as a consequence of divergent dynamics and minimal for in-phase motion due to convergent dynamics.**

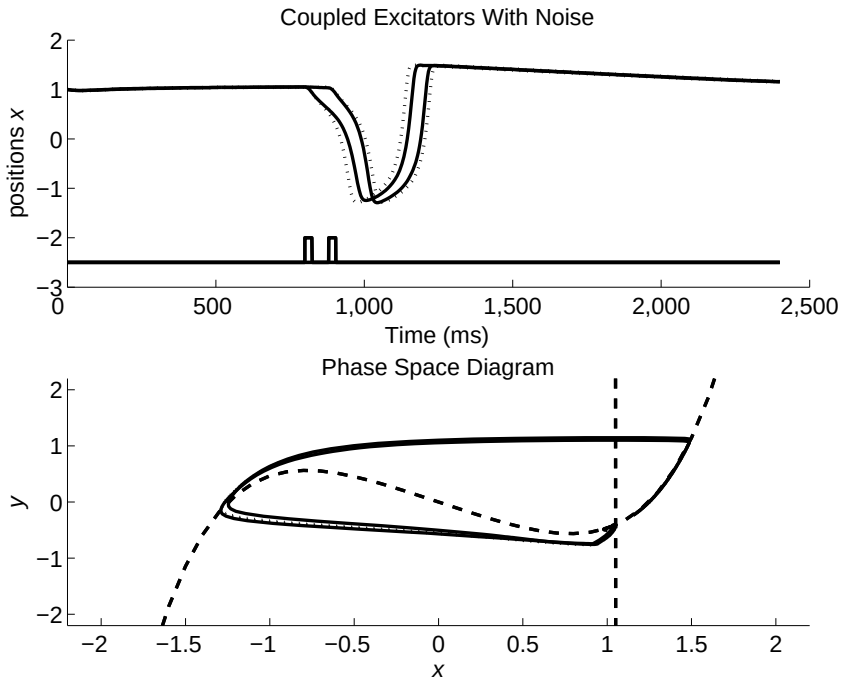


Figure 10: *Convergence.* **The time series of two coupled Excitators (solid lines) and two uncoupled Excitators (dotted lines) following two consecutive stimuli are shown in the top panel. The inter-stimulus interval is 80msec. Each input signal excites only one of the Excitator units. The effect of the coupling is a convergence of the trajectories. The phase space trajectories in x-y-coordinates are plotted in the bottom panel. The dashed lines indicate the nullclines used in the simulation.**

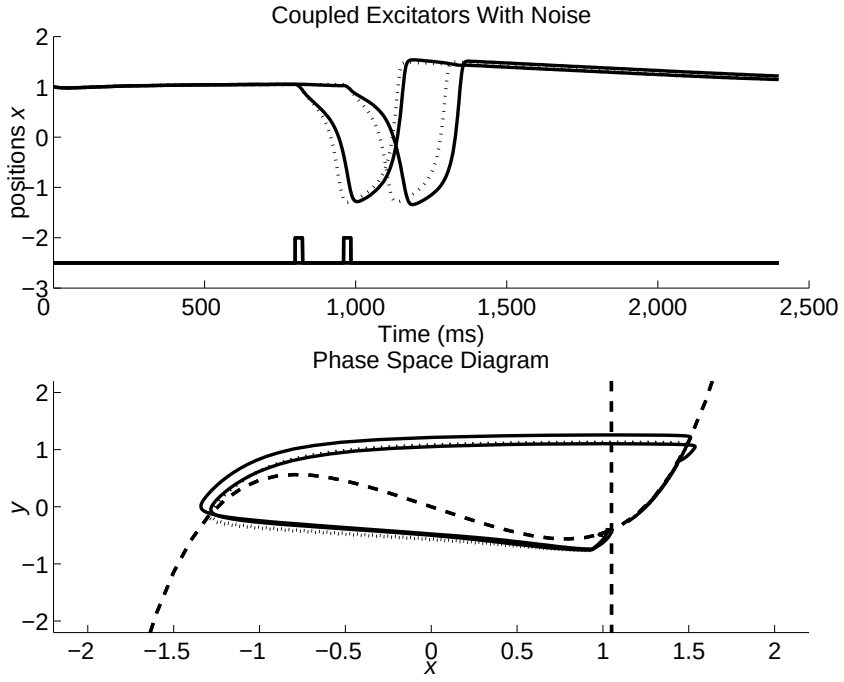


Figure 11: *Divergence.* **The same situation is shown as in figure 10, only the inter stimulus interval between the two inputs is increased to 160msec. The time series in the top panel of the coupled Excitators (solid lines) display a delay compared to the uncoupled Excitators (dotted lines).**

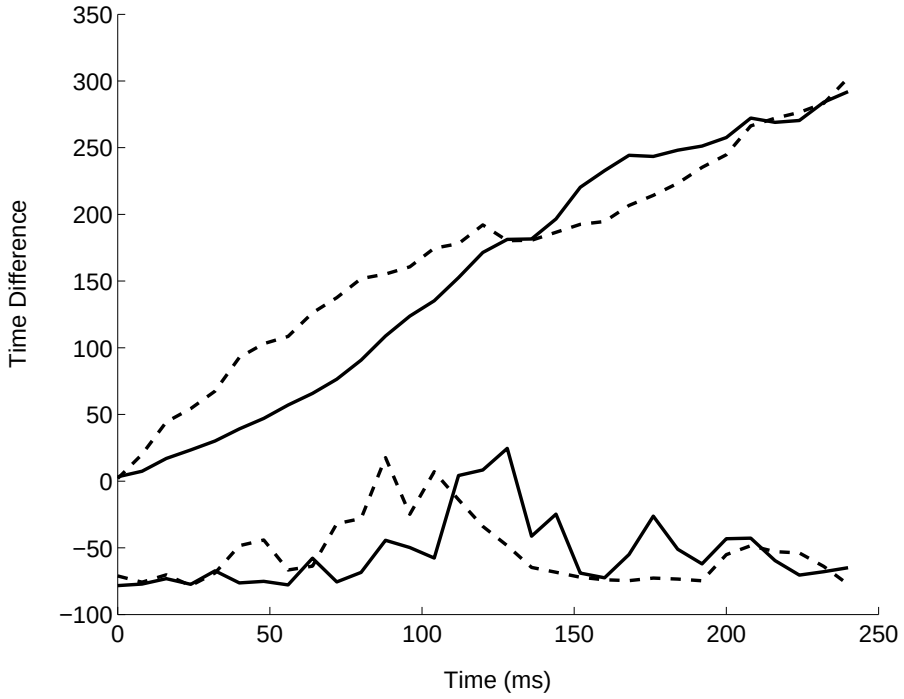


Figure 12: **The mean time difference (upper graphs) and its variance (lower graphs) are plotted as a function of the inter-stimulus interval. The time units are in msec. The dashed lines refer to the uncoupled situation, the solid lines to the coupled situation. The variance is not plotted on the same scale as the time difference graphs. The maximum variance is about 800msec$^2$ at an ISI of approximately 130msec.**